

## The Effect of Different Concentrations of Tellurium on the Structural and Optical Properties of ZnO Nanostructured Films Deposited by Sol-Gel Method

A.U. Sonawane<sup>1</sup>, B.K. Sonawane<sup>2</sup>

<sup>1</sup> DNCVPS Shirish Madhukarrao Chaudhari College Jalgaon, 425001 Maharashtra, India

<sup>2</sup> J.D.M.V.P. Co-Op. Samaj's Arts, Commerce and Science College Jalgaon, 425001 Maharashtra, India

(Received 14 April 2022; revised manuscript received 07 August 2022; published online 25 August 2022)

Undoped and Te-doped ZnO nanostructured films were prepared on glass substrates by a sol-gel technique with different atomic concentrations of Te. The deposited films were characterized to investigate the structural, surface, and optical properties. The films are polycrystalline in nature and have a hexagonal structure. The crystal structure of ZnO<sub>1-x</sub>Te<sub>x</sub> films was determined, and various crystal parameters such as  $2\theta$  value, FWHM, crystalline size, lattice strain, and dislocation density were calculated. The surface morphology of the films was tailored, and it was found that as the doping concentration of Te increases in ZnO, a decrease in the grain size is observed. The transmittance spectra of undoped ZnO and Te-doped ZnO films were highly transparent (~ 80 %) in the visible region. The average transparency was increased to increase the Te doping concentration. Transmittance edges were shifted to lower wavelengths when the atomic percentage of Te concentration increased. When the concentration of Te increased, an increase in the optical band gap of the deposited films was observed. Photoluminescence (PL) shows that all nanofilms have strong peaks in the ultraviolet region and small deep-level emission peaks in the visible region, depending on the Te concentration. The PL spectra of Te-doped ZnO shows a large blue shift from 396 to 381 nm in the UV emission peak position. It was also observed that as the Te doping concentration increased, the intensities of the PL bands in the visible range also increased.

**Keywords:** Sol-gel preparation, Crystal structure, Crystalline size, Lattice strain.

DOI: [10.21272/jnep.14\(4\).04025](https://doi.org/10.21272/jnep.14(4).04025)

PACS numbers: 61.66. – f 81.20.Fw

### 1. INTRODUCTION

Zinc oxide (ZnO) semiconductor material has a wide band gap of 3.44 eV, exciton binding energy of 60 meV, good transparency in the visible wavelength range at room temperature. Therefore, it can be used in the fabrication of various optoelectronic devices such as photodetectors, light-emitting diodes and solar cells [1]. There are mainly two types of nanostructural properties extracted from XRD peak analysis: crystallite size and lattice strain. The change in crystallite size and lattice strain depends on the behavior and concentration of dopant materials [2]. XRD peak position line broadening is used to investigate the dislocation distribution. Normally, doping is used to improve the electrical, structural, and optical properties of pure ZnO thin films to make them suitable for optoelectronic applications [3].

One of the most suitable dopants is Tellurium (Te) in ZnO; Te is a chalcogen family element [4]. Te acts as an anionic dopant in the ZnO lattice and changes its optical properties in the visible spectral region by reducing oxygen vacancies, thus rendering them as a prospective material for next-generation optoelectronic devices [5]. In the present investigation, the synthesis of nanoscale undoped and doped with various concentrations of Te ZnO films with different structural, surface and optical controlled properties is carried out by the sol-gel method on microscopic glass substrates.

### 2. EXPERIMENTAL DETAILS

The starting precursor reagents, solvent and stabilizer used for this deposition method, were zinc acetate dehydrate [(C<sub>4</sub>H<sub>6</sub>O<sub>4</sub>Zn.2H<sub>2</sub>O) Sigma Aldrich-CAS No. 5970-45-6], tellurium tetrachloride [(TeCl<sub>4</sub>) Sigma

Aldrich-CAS No. 10026-07-0], 2-Methoxyethanol [(C<sub>3</sub>H<sub>8</sub>O<sub>2</sub>) Rankem-CAS No. 109-86-4] and Ethanolamine [(H<sub>2</sub>NCH<sub>2</sub>CH<sub>2</sub>OH) Rankem-CAS No. 141-43-5]. 0.45 M solutions were prepared using zinc acetate dehydrate and tellurium tetrachloride powder, which were mixed to formula ZnO<sub>1-x</sub>Te<sub>x</sub> taken at different at. % concentrations  $x = 0, 1, 3, 5$  and  $7$  in 25 ml in 2-methoxy ethanol simultaneously. The solutions were stirred on a magnetic hot plate at ~ 75 °C for 30 min; five drops of ethanolamine were added to each solution. The mixture of solutions was stirred on a magnetic hot plate at a temperature of ~ 75 °C for half an hour; the solutions became transparent and finally aged for 8 h at room temperature.

Before deposition, glass substrates were cleaned with chromic acid and acetone. The films were deposited on a glass substrate using a spin coater. The spin coater speed was maintained at 2000 rpm for 25 s. The coating procedure was repeated twelve times. After each coating, all the films were preheated at 225 °C for 10 min. Finally, samples were post-annealed at a temperature of 350 °C for 1 h in the furnace.

### 3. RESULTS AND DISCUSSION

#### 3.1 XRD

XRD spectra of various Te doping concentrations of 0, 1, 3, 5, and 7 at. % of nanostructured films are shown in Fig. 1a. The XRD spectra show that all deposited films have a hexagonal structure with JCPDS card No. 36-1451. The samples have a high orientation peak (002), indicating that all samples are strongly oriented along the  $c$ -axis. Dominant peaks are oriented at  $2\theta$  values of 31.77°, 34.42°, 36.25°, 47.53°, 56.60°, 62.86° and 67.96° with related XRD peak position of (100),

(002), (101), (102), (110), (103) and (112) planes of the hexagonal structure material. No additional peaks are observed in these spectra, since successful doping of Te into the ZnO lattice occurs without changing the ZnO structure [6].

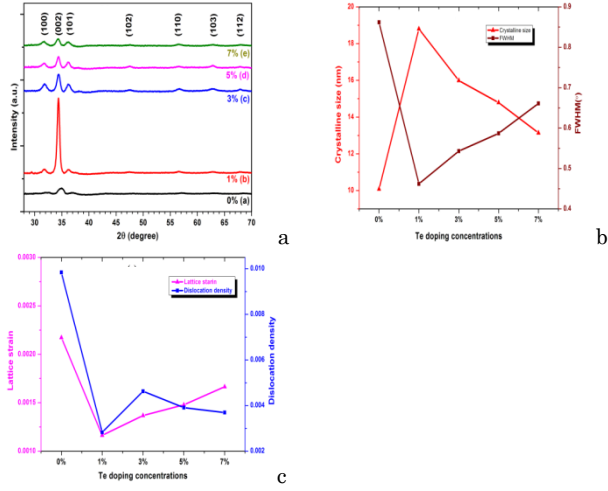


**Fig. 1** – (a) XRD spectra, (b) crystalline size and FWHM, (c) lattice strain and dislocation density of different Te concentrations of  $\text{ZnO}_{1-x}\text{Te}_x$  nanostructured films

It is noticeable from the XRD spectra that the high intensity of the (002) diffraction peak is strongest at 1 % (b) compared to 0 % (a) for undoped ZnO and other different atomic concentrations of Te-doped ZnO films. The intensity of the (002) peak decreases with increasing Te concentration from 1 to 7 at. %. High Te doping concentrations may produce an excess of lattice distortion and subsequently inhibit grain growth. Hence, reduced crystallinity occurs at a high doping percentage of Te-doped ZnO films. These films reveal that the (002) diffraction peak position is shifted towards a smaller angle of  $2\theta$  values compared to 0 % (a). Lattice strain was introduced into the Te-doped ZnO structure due to the main difference in ionic radii of  $\text{Te}^{2-}$  (2.07) and  $\text{O}^{2-}$  (1.40) ions [7].

In the study, the effect of Te doping concentrations on the crystal structure of  $\text{ZnO}_{1-x}\text{Te}_x$  films in various crystal parameters was calculated. The calculated values are listed in Table 1. The crystalline size ( $D$ ) in the (002) diffraction peak of  $\text{ZnO}_{1-x}\text{Te}_x$  films was determined by Scherrer's equation [8]:

$$D = \frac{0.94\lambda}{(\cos\theta)\beta}, \quad (1)$$

where  $\beta$  is the full width at half maximum (FWHM). The calculated crystalline grain sizes at the Te doping concentration from 0 to 7 at. % were found to be 10.08, 18.18, 15.99, 14.79 and 13.14 nm. Fig. 1b shows the crystalline size and FWHM for the (002) peak at different concentrations of  $\text{ZnO}_{1-x}\text{Te}_x$  films. The crystalline size values initially increased and reached their maximum, and then decreased as the Te concentration increased from 0 to 7 at. %. The FWHM value was initially high, then decreased to its lowest value and then increased as the Te concentration increased from 0 to 7 at. %. A smaller FWHM value indicates a better crys-

talline quality of the samples. The resulting FWHM values were attributed to a decrease in crystalline size.

The lattice strain ( $\epsilon$ ) in undoped and Te-doped ZnO films with different atomic concentrations was determined by the following equation [9]:

$$\epsilon = \frac{\beta \cos\theta}{4}. \quad (2)$$

The lattice strain values were found to be 0.001164 to 0.002171, respectively. The dislocation density ( $\delta$ ) was calculated as follows:

$$\delta = \frac{1}{D^2}. \quad (3)$$

The calculated dislocation density values were found to be 0.002829 to 0.009841. The dislocation densities decreased as the Te concentration increased in the ZnO films investigated. Fig. 1c shows the lattice strain and dislocation density of the (002) peak at different Te concentrations of  $\text{ZnO}_{1-x}\text{Te}_x$  films. The lattice strain values were initially high (0 %), decreased to the lowest (1 %), and then increased as the Te concentration increased from 1 to 7 at. %. The dislocation density values were initially maximum (0 %), decreased to the lowest (1 %), then slightly increased (3 %), and finally decreased as the Te concentration increased from 3 to 7 at. %.

**Table 1** –  $2\theta$  values, FWHM, crystalline size, lattice strain ( $\epsilon$ ), dislocation density ( $\delta$ ) and grain size for undoped and Te-doped ZnO nanofilms annealed at 350 °C with different Te doping concentrations

Te doping ratio (at. %)	Peak position $2\theta$ (°)	FWHM $\beta$ (°)	Crystalline size (XRD) $D$ (nm)	Lattice strain $\epsilon$	Dislocation density $\delta$ ( $\text{nm}^{-2}$ )	Grain size (FESEM) (nm)
0	34.42	0.862	10.08	0.00217	0.00984	19.84
1	34.38	0.462	18.80	0.00116	0.00282	26.10
3	34.36	0.543	15.99	0.00136	0.00462	23.67
5	34.32	0.587	14.79	0.00147	0.00391	22.69
7	34.29	0.661	13.14	0.00166	0.00369	22.01

### 3.2 Surface Morphology

Fig. 2(a-e) shows FESEM images for different concentrations of Te-doped ZnO films with different surface morphology and nanocrystalline nature. These micrographs also observe that the surface morphology and shape of undoped ZnO nanostructured films were affected by the Te doping concentration. These images reveal that the grain size changes with increasing Te doping concentration of ZnO films. In Te-doped ZnO images, a decrease in the grain size can be seen on the nanofilm surface with increasing Te concentration, as shown in Fig. 2(b-e).

The grain size of 0, 1, 3, 5, and 7 at. % of Te-doped ZnO nanofilms estimated from FESEM micrographs are 19.84, 26.10, 23.67, 22.69, and 22.01 nm, respectively. Fig. 2f shows 7 at. % Te-doped films with O, Zn, and Te peaks, and the other spectrum appears due to the glass substrate. The EDAX spectra confirmed the successful incorporation of Te element into ZnO films.

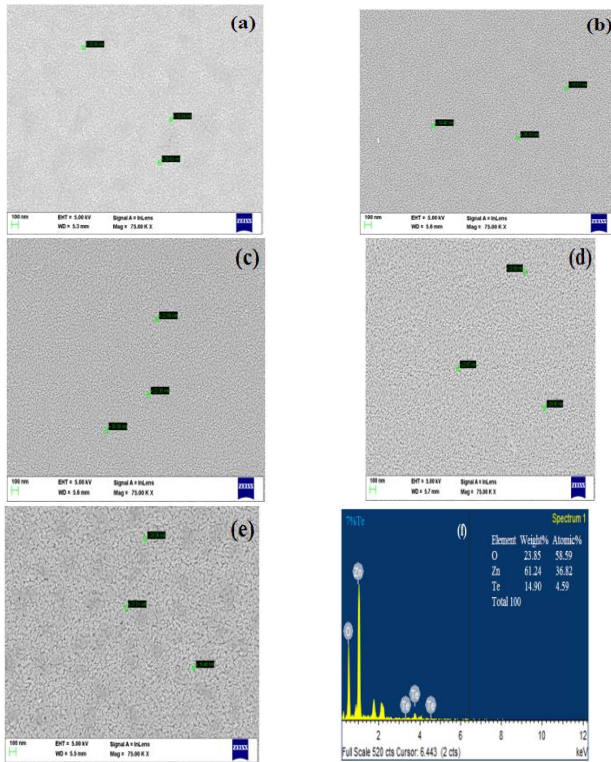


**Fig. 2** – FESEM images of (a) undoped ZnO, (b) 1 at. %, (c) 3 at. %, (d) 5 at. %, (e) 7 at. % Te-doped ZnO; (f) EDAX spectra of 7 %Te-doped ZnO nanocrystalline films

### 3.3 Optical Properties

Fig. 3a shows that optical transmittance spectra for nanostructured films were highly transparent ( $\sim 80\%$ ) in the visible region. A comparison of the transmittance spectra for undoped and different Te-doped ZnO films showed that the average transparency increased with increasing Te doping concentration. Also, the transmittance edges shifted towards lower wavelengths as the atomic percentage of the Te concentration increased. The decrease in the transmittance spectra with increasing Te doping may be due to light scattering at grain boundaries [10]. Optical band gap energies ( $E_g$ ) of undoped and Te-doped nanostructured ZnO films were determined using Tauc's formula as follows [11]:

$$(ah\nu)^2 = A(h\nu - E_g). \quad (4)$$

Fig. 3b shows that optical band gap energy  $E_g$  values increase with an increase in the Te doping concentration. Films with Te concentrations of 0, 1, 3, 5, and 7 at. % have the corresponding band gap values of 3.215, 3.223, 3.245, 3.275, and 3.290 eV. The optical band gap energies of the variation in Te-doped ZnO films were blue-shifted upward due to the MB effect [12].

### 3.4 Photoluminescence

The effect of undoped and Te-doped (with different concentrations) nanostructured ZnO films is studied using photoluminescence (PL) spectra. With an excitation wavelength of 330 nm, the measured PL spectra at room temperature for all nanofilms are shown in Fig. 4. The PL spectra of undoped and Te-doped ZnO nanofilms

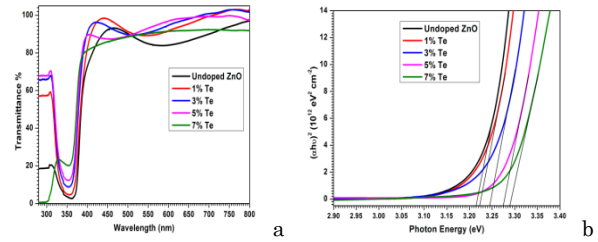


**Fig. 3** – (a) Optical transmittance spectra, (b)  $(ah\nu)^2$  vs  $h\nu$  plot for  $\text{ZnO}_{1-x}\text{Te}_x$  nanocrystalline films at different Te doping concentrations

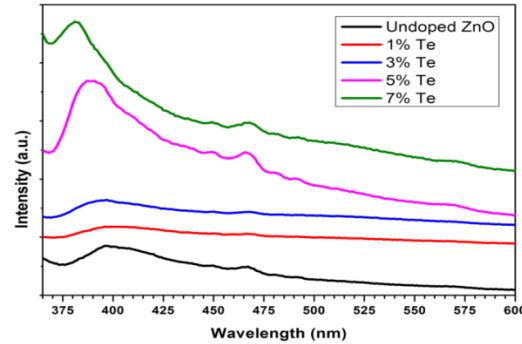


**Fig. 4** – PL spectra for different doping concentrations of Te-doped ZnO nanofilms

exhibit strong peaks in the ultraviolet (UV) region and small deep level emission peaks in the visible region. We compared with undoped ZnO nanostructure films, the PL spectra of Te-doped ZnO show a large blue shift from 396 to 381 nm in the UV emission peak position; this supports the shift of the optical band gap in these samples and the XRD results on different doping concentrations of Te in the ZnO structure [13].

It was found that in undoped and 1 % Te-doped ZnO nanofilms, the PL emission intensity was lowest, since Te is incorporated into the ZnO crystal lattice in the form of an interstitial point defect. It was also observed that as the Te doping concentration increases from 1 to 7 at. %, the intensity of PL bands in the visible range increased because Te doping percentage changes the relative concentration of intrinsic defects. These types of defects in the ZnO structure with Te doping provide better utilization of materials in visible light. We observed that as the atomic concentration of Te increased, the intensities of the broad luminescence bands also increased. These results can be used in optoelectronic applications [14, 15].

## 4. CONCLUSIONS

XRD patterns showed that all nanostructures are polycrystalline in nature with a hexagonal structure and have a preferential orientation along the (002) plane. The FWHM, crystalline grain size, lattice strain, and dislocation density of films are affected by different Te doping concentrations. The FESEM images show that the surface morphology and shape of undoped ZnO nanoparticles change with different Te doping concentrations. In Te-doped ZnO images, one can see a decrease in grain size on the surface of nanostructured films with increasing Te concentration. Te incorporation is confirmed by EDAX investigations. The trans-

mittance of the deposited nanofilms is found to be very high. The band gap values of the films increase with increasing Te concentrations in the ZnO structure. When studying the PL spectra of undoped and Te-doped (with different lower concentrations) nanocrystalline ZnO films, strong peaks in the ultraviolet region and small deep level emission peaks in the visible re-

gion are observed. It is also found that as the Te doping concentration increases from 1 to 7 at. %, the intensity of the PL bands in the visible range increases because Te doping percentage changes the proportional concentration of intrinsic defects. We believe that these results for Te-doped ZnO can be used in nanoscale optoelectronic applications.

## REFERENCES

1. S. Saira, A. Shaari, *Optik* **206**, 164285 (2020).
2. P. Bindu, S. Thomas, *J. Theor. Appl. Phys.* **8**, 123 (2014).
3. R. Mohamed, A.S. Ismail, *AIP Conf. Proc.* **1733**, 020061 (2016).
4. W. Wu, G. Qiu, *Chem. Soc. Rev.* **47**, 7203 (2018).
5. J. Guo, J. Zhao, D. Huang, Y. Wang, *Nanoscale* **11**, 6235 (2019).
6. A.K. Tareen, K. Khan, *Nanoscale* **13**, 510 (2020).
7. S. Akin, E. Erol, *Electrochim. Acta* **225**, 243 (2017).
8. R. Pandey, S. Yuldashev, *Curr. Appl. Phys.* **12**, S56 (2012).
9. C.K. Kasar, U.S. Sonawane, D.S. Patil, *J. Mater. Sci.* **27**, 11885 (2016).
10. M. Shkir, S.S. Shaikh, S. AlFaify, *J. Mater. Sci.* **30**, 17469 (2019).
11. T. Hurma, M. Caglar, *Mater. Sci. Semicond. Proc.* **110**, 104949 (2020).
12. Z. Qiuxiang, L. Junfeng, *Sci. Rep.* **6**, 36194 (2016).
13. S. Sönmezoğlu, E. Akman, *Appl. Surf. Sci.* **318**, 319 (2014).
14. N. Shakti, C. Devi, A.K. Patra, P.S. Gupta, *AIP Adv.* **8**, 015306 (2018).
15. X. Li, X. Zhu, K. Jin, D. Yang, *Opt. Mater.* **100**, 109657 (2020).

## Вплив різних концентрацій телуру на структурні та оптичні властивості наноструктурованих плівок ZnO, нанесених золь-гель методом

A.U. Sonawane<sup>1</sup>, B.K. Sonawane<sup>2</sup>

<sup>1</sup> DNCVPS Shirish Madhukarrao Chaudhari College Jalgaon, 425001 Maharashtra, India

<sup>2</sup> J.D.M.V.P. Co-Op. Samaj's Arts, Commerce and Science College Jalgaon, 425001 Maharashtra, India

Нелеговані та леговані Te наноструктуровані плівки ZnO були виготовлені на скляних підкладках золь-гель методом з різними атомними концентраціями Te. Проведені дослідження їх структурних, поверхневих та оптичних властивостей. Плівки полікристалічні за своєю природою і мають гексагональну структуру. Було визначено кристалічну структуру плівок ZnO<sub>1-x</sub>Te<sub>x</sub> і розраховано різні кристалічні параметри, такі як значення  $2\theta$ , FWHM, розмір кристалітів, деформація ґратки та густина дислокацій. При вивченні морфології поверхні плівок встановлено, що зі збільшенням концентрації легування Te в ZnO спостерігається зменшення розміру зерен. Спектри пропускання нелегованих плівок ZnO та плівок ZnO, легованих Te, високопрозорі (~ 80 %) у видимій області спектру. Середня прозорість зростає при збільшенні концентрації атомів Te. Краї пропускання були зміщені в бік менших довжин хвиль, коли атомний відсоток концентрації Te збільшувався. При збільшенні концентрації Te спостерігалось збільшення оптичної забороненої зони нанесених плівок. Фотолюмінесценція (ФЛ) показує, що всі наноплівки мають сильні піки в ультрафіолетовій області та невеликі глибокі піки випромінювання у видимій області залежно від концентрації Te. Спектри ФЛ плівок ZnO, легованих Te, демонструють велике сине зміщення від 396 до 381 нм у положенні піку УФ-випромінювання. Також встановлено, що зі збільшенням концентрації легування Te зростає інтенсивність смуг ФЛ у видимому діапазоні.

**Ключові слова:** Золь-гель приготування, Кристалічна структура, Розмір кристала, Деформація ґратки.